Chapter 3

Seismic Hazard Assessment and Source Zone Delineation in Northeast India: A case study of the Kopili Fault Region and its Vicinity

Chapter 3

Seismic Hazard Assessment and Source Zone Delineation in Northeast India: A case study of the Kopili Fault Region and its Vicinity

3.1. Introduction

Northeastern India, located in Southeast Asia, is a region with significant seismic activity due to its diverse geological formations. The region is designated as zone V on the national seismic zoning Map of India [1] and is home to the Eastern Himalayas, IBR, Bangladesh, and Andaman and Sumatra. The region has been witnessing several earthquakes, which are frequent due to the complex tectonic setting. Numerous faults in the area originated around fifty million years ago when the Indian plate slipped beneath the Eurasian plate [2]. The ongoing collision and subduction between these plates contribute to the region's high seismic activity in the northern frontier of India [3]. The Kopili fault, which runs in a Northwest to Southeast direction and traverses the central part of the Assam state, is widely believed to be the source of significant earthquakes that occurred in the region. Large historical earthquakes of magnitude seven or higher, which have occurred in the Kopili fault zone, are characteristic of an active Kopili fault [4]. These earthquakes have not only wreaked havoc in the northeastern region of India but have also altered the pattern of seismic activities around the fault in past times. Determining seismic hazard at the regional level is crucial for the architectural design of structures and reducing losses in terms of human lives and physical property.

Probabilistic or deterministic seismic hazard analysis can be used to determine the likelihood of various earthquake-induced motion parameters for a given site or region. This approach offers a comprehensive view of the entire range of earthquake activity in the analyzed Seismotectonic region and allows for assessing the relative impact of different earthquake prone zones on the overall seismic risk of a particular location.

Sharma, V. and Biswas, R. Seismic hazard assessment and source zone delineation in Northeast India: a case study of the Kopili fault region and its vicinity. Indian Geotechnical Journal, 54: 598–626, 2024.

This chapter intends to produce a Seismotectonic map for the Kopili fault and its vicinity, addressing the challenges of constructing a Seismotectonics map for a specific area. By encompassing diverse regions, the seismic study may yield heterogeneous results, making it challenging to establish consistent patterns or relationships across the entire area. Region-specific

studies offer a more detailed and contextually relevant understanding of seismic hazards, enabling a targeted approach to risk assessment, mitigation, and preparedness.

3.2. Tectonic setup

The Kopili Shear Zone, a fault in the Himalayas, spans almost 300 km in length and 50 km in width (as shown in Figure 3.1). It is named after the Kopili River, an affluent of the Brahmaputra River [5]. The Kopili lineament is an active fault due to its significant seismic activity. The Kopili fault can be traced through three major tectonic regions: the lower Assam Valley, eastern Himalayan ranges, and the Arakan-Yoma suture zone. The Indian and Eurasian tectonic plates collided approximately sixty million years ago, leading to the formation of the Himalayas. The Himalayan region comprises various folds, faults, and thrusts, including the Indus Suture Thrust (IST), Main Central Thrust (MCT), and Main Boundary Thrust (MBT). The MBT acts as a demarcation between the Lesser Himalayas and the Greater Himalayas, while the MCT serves as the dividing line between the Lesser Himalaya and the Central Himalaya [6]. Seismic gaps have been observed in the Northeastern Himalayan region along the MBT or MCT, indicating potential for future earthquakes. The Kopili fault extends beyond the MBT and MCT, with the Shillong plateau, located to the west of the Kopili fault, moving eastward along the Dauki fault (DF) by approximately 300 kilometers. The Mikir Hills massif, located to the east of the Shillong plateau, has geological features similar to those of the Shillong plateau but on opposite sides of the seismically active region characterized by the NW-SE trending Kopili fault. The Shillong Plateau is different from the rocks in the southwest due to the presence of the Dapsi thrust (DT), an extension of the DF running from north to southeast. The Indo-Myanmar mountains, located east and south of the Assam Valley, were formed by the collision of Indian and Burmese tectonic plates. The mountains consist of multiple thrust fault systems, with the most notable being the Naga-Disang thrust (NDT), Churachandpur-Mao fault (CMF), Kaladan fault, and Kabaw fault (KF). The northern segment of the

Kaladan fault has strike-slip faulting, while the southern part exhibits a thrust focal mechanism. The region is distinguished by sedimentary rock strata arranged in a trough shape, with sediment depths reaching up to twenty kilometers. The low seismicity of the region can be attributed to thick sediment deposits and the majority of earthquakes occurring within the same tectonic plate. The major fault in the Bengal basin is the strike-slip Sylhet fault (SF), which was the epicenter of the 1918 Srimangal earthquake. The Eocene Hinge Zone (EHZ), spanning 500 km and 25 km, is another significant tectonic feature in the region [7]. The Himalayas can be seen when traveling north of the eastern part of the Bengal basin. Within the specified 300 km radius centered at Tezpur city, a total of 36 tectonic sources have been identified. The research specifically concentrates on linear tectonic features because of their even distribution throughout the area. Using the data collected on these features, a detailed source map of all faults in the seismotectonic region has been constructed, as depicted in Figure 3.1.

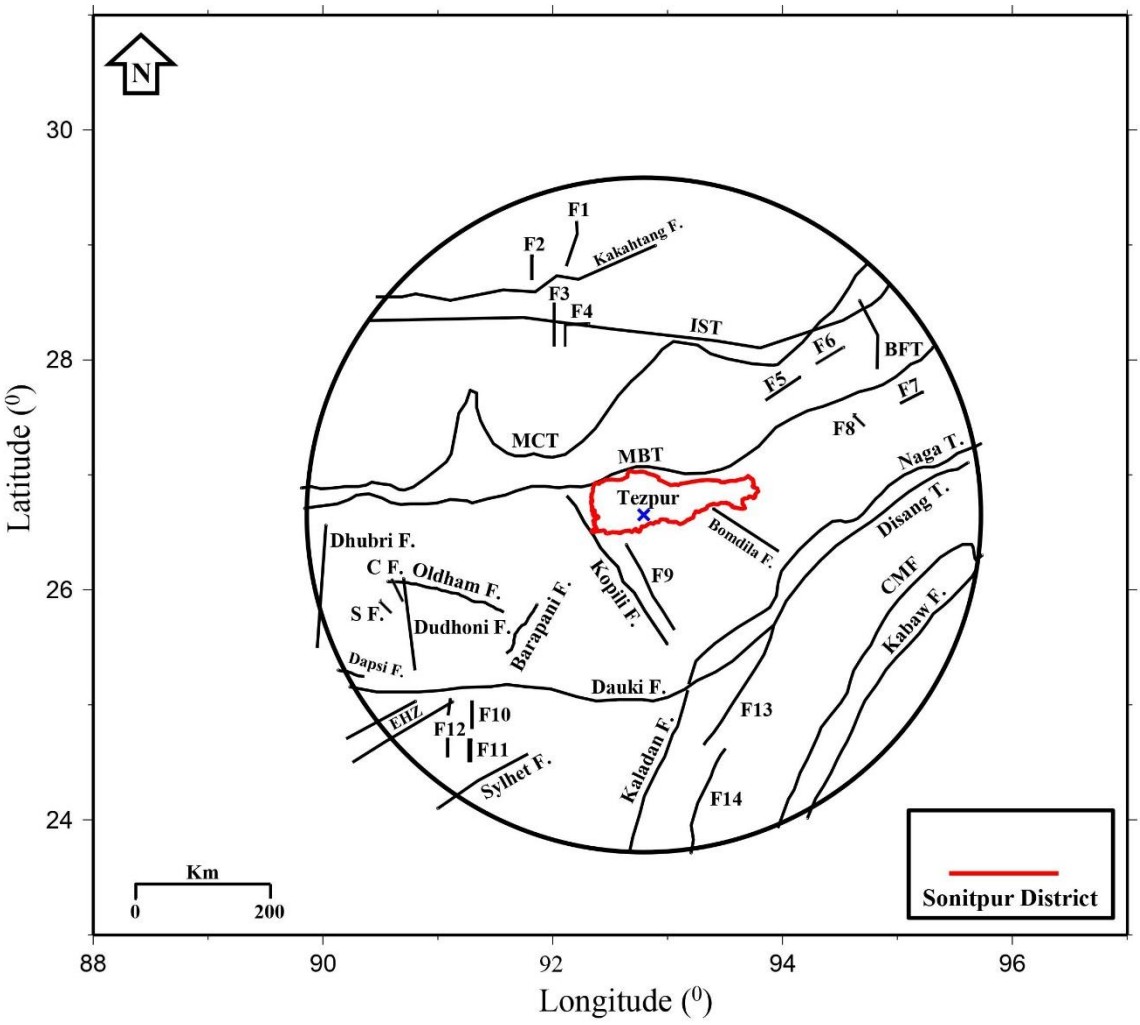

Figure 3.1. The tectonic plot of the study region consisting of all the faults are also included. The blue mark shows the epicentral location of Tezpur, Sonitpur district, Assam, India.

3.3. Compilation of Earthquake catalog for the study region

To understand the seismic activity of the study area, we compiled a comprehensive earthquake database from 825 to 2023 within a 300 km radius. This database included historical and instrumental earthquakes sourced from the USGS, the ISC, the National Disaster Management Authority (NDMA), and the India Meteorological Department (IMD). By integrating data from these sources, we created a unified dataset of 4008 earthquake events across various magnitude scales namely surface magnitude scale (M_S), duration magnitude scale (M_D), local magnitude scale (M_L), moment magnitude scale (M_W), and body magnitude scale (mb). This dataset forms the basis for assessing the seismic hazard posed by the Kopili fault and its vicinity. The entire earthquake database is converted to the Mw scale using the conversion formula by [8] (as mentioned in Table 2.1 of chapter 2). The database was refined to 3608 distinct earthquake events, focusing on independent mainshocks through declustering. The [9] method was most effective, identifying 3525 declustered events and 38 clusters, enhancing seismic hazard assessments.

3.4. Analysis of Seismic Activity, Estimating Maximum Magnitude (M_{max}), and Zoning Seismic Sources in the Study Area

Numerous studies have been conducted to assess seismic hazards in Northeast India, dividing the region into different source zones using various methodologies. [10], [11], [12], [13], [14], [8], [15], [16], [5], and [17], and have all contributed to the identification of potential seismic zones in India and neighboring regions. However, variations in methodologies and considerations have led to differences in the identified source zones. The present study region is subdivided into four seismic zones: the NEHSZ, SASZ, BSSZ, and IBSTZ. The division of the study region is influenced by the findings of [2]. To construct a seismotectonic plot of the Kopili fault and its surrounding area, the seismic and tectonic sources identified and utilized in this research are as follows:

1) North-Eastern Himalayan Seismic Zone (NEHSZ)

The NEHSZ is a seismic zone in the northeastern part of the Himalayan range, known for its high seismic activity. It extends across various states in the northeast Indian region and is influenced by the collision of the Indian subcontinental plate with the Eurasian lithospheric Plate, leading to intense tectonic activity and frequent earthquakes. The NEHSZ is associated with several active faults and thrust systems, such as the IST, MCT, and MBT, which contribute to seismic hazards in the region. The IST marks the boundary between the Indian and Eurasian plates, resulting from complex tectonic processes that have shaped the region over millions of years. The MCT represents the detachment surface where rocks from the Lesser Himalayas were thrust over the rocks of the Higher Himalayas, resulting in highly deformed and metamorphosed rocks. Over time, tectonic activity and erosion have exposed the MCT and associated structures, providing valuable insights into the tectonic history and evolution of the Himalayan region. The MBT represents the prominent discontinuity between the sub-Himalayan and lesser Himalayan zones, characterized by intense seismic activity and devastating earthquakes. The Eastern Himalayas are characterized by predominantly convergent plate movements in the mountain ranges, with an average convergence rate estimated at around 20 millimeters per year. However, there has been an increase in the rate of convergence in specific regions, with the typical range of convergence in the northeastern Himalayan region falling between 15 to 20 millimeters per year, except for the eastern Assam region where the convergence rate reaches up to 31 millimeters per year [18].

2) Shillong-Assam Seismic Zone (SASZ)

The SASZ in northeastern India is characterized by diverse geology and tectonic features. The region is part of the larger Indo-Burmese orogenic belt, influenced by major faults and thrusts such as the DF, Oldham fault (OF), and Kopili fault. The Shillong Plateau, primarily composed of sedimentary, metamorphic, and volcanic rocks, experiences minimal tectonic deformation. The Assam Valley, on the other hand, is predominantly covered by alluvial deposits, including sand, silt, and clay, brought down by major rivers like the Brahmaputra. The Shillong Plateau is considered a stable block within the region, experiencing minimal tectonic deformation. In contrast, the Assam Valley is characterized by active tectonic processes, including compression and thrusting along major faults. The Kopili fault has been identified as an active fault zone with significant seismic activity. The Shillong Plateau is an elevated region primarily composed of crystalline rocks, with a 300 km eastward shift along the DF. The Kopili lineament separates the Shillong Plateau

and the adjacent Mikir hills, with the Dapsi thrust (DT) being a significant thrust fault within the region. The Assam valley area has experienced a significant earthquake event with a maximum recorded magnitude of 8.6 on June 26, 1897, with a largest time interval between occurrences of large earthquakes with a magnitude of 7.0 or higher being 26 years. Recent research [19] indicates that the Shillong plateau and the Assam Valley have undergone detachment from the Indian plate, consisting of distinct, rigid blocks known as the Shillong and Assam blocks. The central region of the Shillong Plateau and certain locations north of the plateau within the Assam Valley exhibit characteristics of a rigid block, with a southward motion of approximately 7 milometers per year in relation to the fixed Indian plate [20].

3) Bengal Subsurface Seismic Zone (BSSZ)

The Bengal Basin is a geologically complex region in the northeastern part of the Indian subcontinent, characterized by a large sedimentary basin across Bangladesh and parts of West Bengal. It is part of the larger Bengal Basin-Sylhet Trough region, influenced by the convergence and subduction of the Indian Plate beneath the Eurasian Plate. The basin is considered a passive margin, not currently experiencing significant tectonic activity. The geological history of the Bengal Basin has been shaped by previous tectonic events, such as the collision between the Indian Plate and the Eurasian Plate, leading to the uplift of the Himalayas and the creation of the Indo-Gangetic Plain. The basin's sedimentary deposits are of great significance for understanding past climate changes and the region's environmental history. The BSSZ is situated west of the IBSTZ, with lower seismic activity compared to other zones. However, intraplate earthquakes have been documented within the BSSZ, such as the 1918 Srimangal earthquake and the 1935 Pabna earthquake. The EHZ, a narrow and elongate zone separating post-Eocene sediments from the shelf zone, is believed to mark the boundary between the continental crust and the young oceanic crust [21].

4) Indo-Burma Seismic Thrust Zone (IBSTZ)

The IBSTZ is located in the eastern and southeastern parts of the SASZ and includes the Indo-Burmese ranges. The region is home to several faults, including the NDT, which play a significant role in the tectonic framework and have influenced its geological evolution.

The Naga Fault is an east-west trending fault that runs through Nagaland and Manipur, contributing to the formation of the Naga Hills and Manipur Hills, part of the larger Patkai Range. The Disang Fault, also known as the Dhansiri Disang Fault, is a reverse fault characterized by vertical movement and has influenced the development of the Disang Group of rocks. These fault systems have implications for seismic activity and earthquake hazards in the region. Earthquakes associated with these faults can occur due to the release of accumulated strain from ongoing tectonic forces. The Kaladan fault extends from the southern Arakan coast with thrust faulting to the northern Nagaland region, while the Central Myanmar Fault exhibits strike-slip faulting in the Imphal valley. The KF, 280 km long and characterized by strike-slip faulting, is located to the east of the Central Myanmar Fault and has the potential to produce even larger magnitude earthquakes in the future. The Indo-Burmese Mountain ranges exhibit a distinct tectonic movement pattern, with most faults in the studied region exhibiting strike-slip motion [22]. The region is experiencing convergence at a rate of approximately 11.6 ± 5.4 millimeters per year, and has the potential to generate earthquakes of magnitude 8.2 or higher [23]. Thus, the seismic-tectonic zone is categorized into four well-defined zones: NEHSZ, SASZ, BSSZ, and IBSTZ (as shown in Figure 3.2).

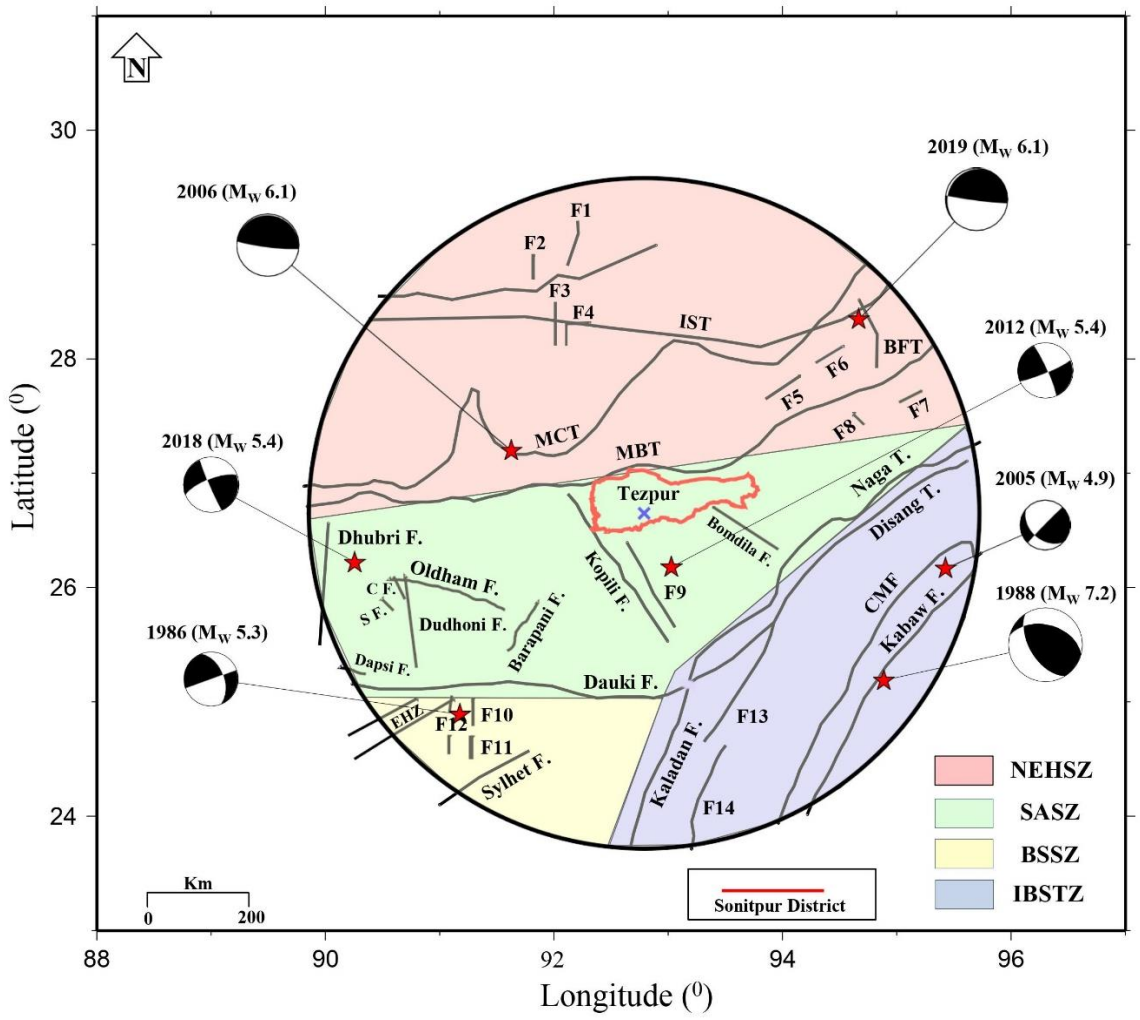

Figure 3.2. The Seismotectonic plot of the study region consisting of four different seismic zones namely: NEHSZ, SASZ, BSSZ, and IBSTZ.

3.5. Seismicity analysis and Estimation of seismic parameters

The earthquake data is examined by dividing it into four separate seismic zones. This division allows for the assessment of completeness within each zone and provides insights into how they impact the Seismic vulnerability of the Kopili fault and its surrounding area. To evaluate the completeness in terms of magnitude and time, thorough analyses are performed for each of the four distinct seismic zones, as described in the following subsections.

3.5.1. Earthquake magnitude completeness test

The estimation of M_C is a crucial step in ensuring data completeness during investigations. In this chapter, the M_C of the earthquake catalog was assessed using the MAXC method [24], with a correction factor of '+ 0.2' added to the M_C value [25]. The M_C values for the complete earthquake catalog and each seismic zone were estimated using the earthquake catalog compiled at moment magnitude scale (M_W) scale and Das magnitude scale (M_{Wg}). The M_C values for the entire study region, NEHSZ, SASZ, BSSZ, and IBSTZ were determined to be 4.1 respectively (Figure 3.3).

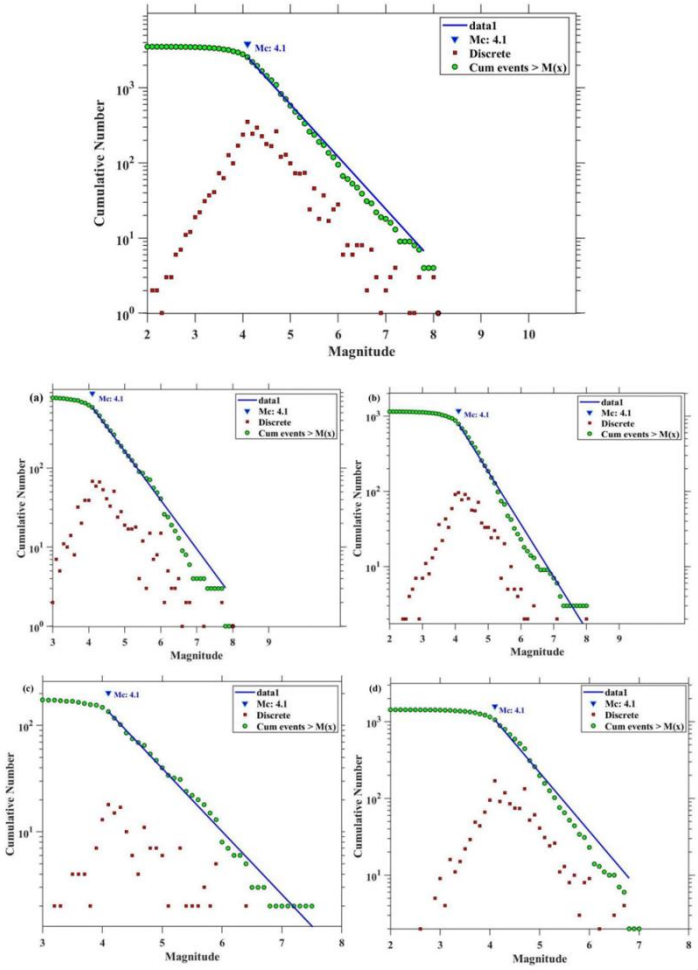

Figure 3.3. The FMD curve showing M_C for different earthquake catalog including Complete catalog for study region a) NEHSZ b) SASZ c) BSSZ and d) IBSTZ using M_W scale.

Similarly, Figure 3.4 shows the M_C values for the entire earthquake catalog and four distinct seismic source zones using the M_{Wg} scale. The M_C values are 3.7 for each region, with a 0.4 difference observed between the M_W and M_{Wg} scaled earthquake catalogs.

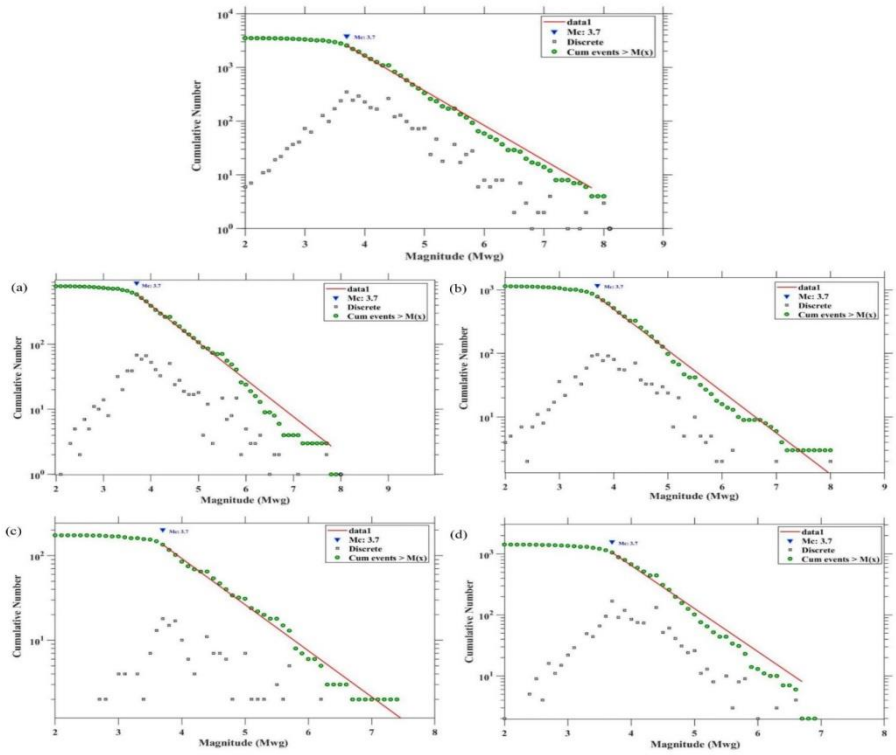

Figure 3.4. The FMD curve showing M_C for different earthquake catalog including Complete catalog for study region a) NEHSZ b) SASZ c) BSSZ and d) IBSTZ using M_{Wg}.

Overestimation and underestimation of the M_C in seismic studies can lead to incomplete understanding of seismic behaviour and underestimated seismic risks. Overestimating the M_C can exclude smaller earthquakes, while underestimating it can overwhelm the dataset and make it difficult to discern meaningful patterns. Striking the right balance in determining the M_C is crucial for accurate seismic analysis and hazard assessment. The M_W scale can resolve these issues, as earthquakes with a magnitude of 4 or greater are significant for seismic hazard analysis [2]. Analysts often consider earthquakes with magnitudes below 4 inconsequential, but focusing on larger earthquakes allows for more efficient allocation of resources. Therefore, the M_C value obtained using the M_W scaled earthquake catalog is used for further analysis, considering the specific threshold for insignificance varies depending on the analysis objectives and seismic activity levels.

3.5.2. Earthquake catalog temporal completeness test

The completeness method, introduced by [26], is used to analyse the earthquake catalog, addressing challenges in establishing earthquake recurrence relations. Table 3.1 lists the time periods during which completeness is achieved for various magnitude ranges in each of the four distinct earthquake zones. The temporal completeness plot for four different earthquake catalogues assigned to four earthquake zones can be seen in Figure 3.5.

Table 3.1. The temporal and magnitude completeness for different zones.

S.No.	Seismic Zone	M_C	Range	Completeness period (years)
1	NEHSZ	4.1	$4.1 \leq M_W \leq 5.0$	40
			$5.1 \leq M_W \leq 6.0$	110
			$6.1 \leq M_W \leq 7.0$	150
			$7.1 \leq M_W \leq 8.0$	230
2	SASZ	4.1	$4.1 \leq M_W \leq 5.0$	40
			$5.1 \leq M_W \leq 6.0$	100
			$6.1 \leq M_W \leq 7.0$	120
			$7.1 \leq M_W \leq 8.0$	150
			$M_W \geq 8.1$	230
3	BSSZ	4.1	$4.1 \leq M_W \leq 5.0$	40
			$5.1 \leq M_W \leq 6.0$	70
			$6.1 \leq M_W \leq 7.0$	140
			$7.1 \leq M_W \leq 8.0$	170
4	IBSTZ	4.1	$4.1 \leq M_W \leq 5.0$	40
			$5.1 \leq M_W \leq 6.0$	100
			$6.1 \leq M_W \leq 7.0$	120
			$7.1 \leq M_W \leq 8.0$	150

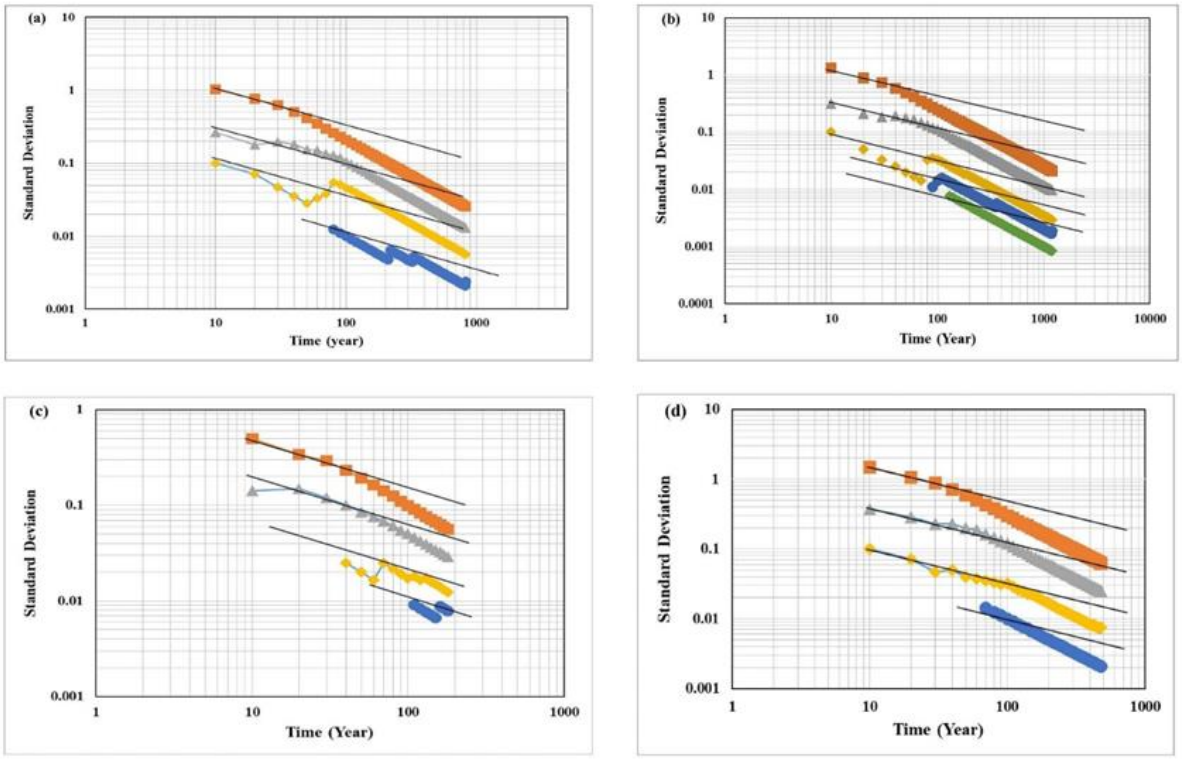

Figure 3.5. The temporal completeness plot for different catalogues of four distinct seismic zones namely a) NEHSZ b) SASZ c) BSSZ d) IBSTZ.

As mentioned above, for accurate and reliable seismic hazard analysis, it's crucial to have a dataset of uniform, homogeneous, and complete events. Uniformity ensures even distribution across the study area, homogeneity means events have similar characteristics, and completeness includes all significant events above a certain magnitude. This comprehensive dataset facilitates understanding seismic activity and identifying potential hazards. Figure 3.6 shows a tectonic plot of the region with events meeting these criteria, used for estimating seismic hazard attributes in the four distinct seismic zones.

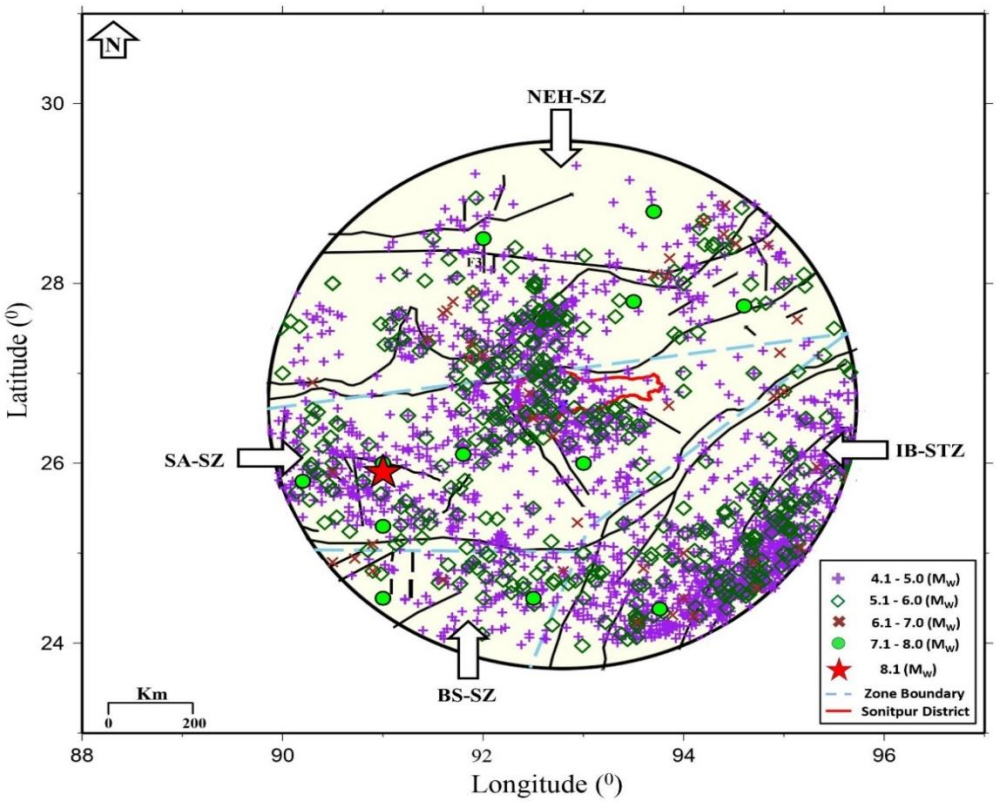

Figure 3.6. The epicentral location of the uniform, declustered, homogenous and complete data set. The four seismic zones are as follow: NEHSZ, SASZ, BSSZ, and IBSTZ.

3.5.3. Estimation of seismic hazard parameters

After analysing earthquake catalogs for the four seismic zones, we estimated the b-value for each zone using two methods: the [27] method and the [28] method. The [27] method uses least-squares fitting to estimate the b-value, representing the rate of decrease in earthquake frequency corresponding to increasing magnitude. The [28] method incorporates regional variations and considers both pre-instrumental and instrumental earthquake data for a comprehensive estimation. The GR method, however, doesn't account for the M_C, a limitation addressed in this study using the [28] method. This method, based on MLE, divides the earthquake catalog into an extreme catalog (pre-instrumental data) and a sub-complete catalog (instrumental data), each with different minimum magnitude thresholds. Using the [28] method, we estimated the seismicity rate (λ), b-value, β (2.303 times b), and maximum magnitude (Mmax) for each zone. The MAXC method was applied to determine M_C for each catalog. The resulting values for λ, b, β, and Mmax for the four seismic zones are summarized in Table 3.2, providing comprehensive insights into the seismic characteristics of each zone.

Table 3.2. The seismic parameters (a, b-value, λ, β and Mmax) are listed for the study region.

Seismic Zone	a-value	b-value	λ	β	Mmax (observed)	M_{max} [28]
NEHSZ	4.43	0.83 ± 0.04 (Present Analysis) 0.66 ± 0.04 [17] 0.89 ± 0.03 [2] 0.70 ± 0.04 [14] 0.71 ± 0.04 [29] 1.05 ± 0.06 [30]	5.34 ± 0.74	1.91 ± 0.08	8	8.11 ± 0.51
SASZ	4.99	0.91 ± 0.04 (Present Analysis) 0.8 ± 0.05 [17] 0.91 ± 0.03 [2] 0.67 ± 0.07 [14] 0.73 ± 0.04 [29]	6.92 ± 1.36	2.09 ± 0.08	8.1	8.60 ± 0.52
BSSZ	3.83	0.81 ± 0.07 (Present Analysis) 0.69 ± 0.05 [17] 0.80 ± 0.03 [2] 0.69 ± 0.08 [14] 0.74 ± 0.04 [29]	3.05 ± 0.66	1.86 ± 0.17	7.6	8.10 ± 0.91
IBSTZ	5.23	0.94 ± 0.03 (Present Analysis) 0.85 ± 0.03 [17] 0.94 ± 0.02 [2] 0.86 ± 0.03 [14] 1.17 ± 0.04 [30]	11.45 ± 1.71	2.17 ± 0.07	7.2	7.70 ± 0.50

Comparing the b-values from previous research and this study, we find variations due to differences in study region size, earthquake catalog duration, M_C values, and calculation methods. However, the b-values from this study align with those estimated by [2] for the analyzed seismic zones. Additionally, other seismic hazard constraints, such as the most probable maximum annual earthquake and the probability of different magnitudes occurring over time, are estimated using GEV method.

3.6. Results and Discussion

[30] determined the maximum magnitude values in four earthquake zones, finding the highest b-value in the Eastern Boundary Zone (EBZ), including the Indo-Burma subduction zone. Our study also found the highest b-value in the Indo-Burma seismic thrust zone, though specific values differed due to variations in earthquake catalog duration and seismic zonation approach. Similar results were reported by [14], [15], and [2]. [17] divided northeast India into six seismic zones, finding the highest a-values and b-values in the Indo-Burma subduction zone, indicating high seismic activity and a predominance of smaller earthquakes. Our study confirms these findings, showing the Indo-Burma seismic thrust zone with the highest a-values and b-values, suggesting frequent, lower magnitude events. Variations in values can be attributed to differences in estimation methods, study region extents, and earthquake catalog durations. The maximum magnitude (Mmax) for NEHSZ, SASZ, BSSZ, and IBSTZ was estimated using [28], resulting in values of 8.11 ± 0.51, 8.60 ± 0.52, 8.10 ± 0.91, and 7.70 ± 0.50, respectively. [2] also used this method but reported different Mmax values, likely due to variations in earthquake catalog duration and seismic zone boundaries.

3.6.1. Gumbel Extreme Value Theory: Understanding Extreme Event Analysis

The study employed GEV theory to evaluate earthquake hazard characteristics in the designated study areas. The region of interest was divided into four primary seismogenic source zones, considering factors such as seismic activity, tectonic features, and earthquake focal mechanisms. To appraise the seismic risk, a comprehensive and reliable database of seismic events was utilized, allowing for the estimation of H(t), T(m), and P(t) at different locations.

3.6.2. Estimation of most likely extreme seismic magnitudes

Table 3.3 presents the GR parameters ('a'; 'b') for the four delineated zones, which were used for the evaluation of Gumbel parameters ('α'; 'β') with equation 5 (mentioned in Chapter 2). Using these parameters in equation 12 (mentioned in Chapter 2), the most probable largest annual magnitude (H) was calculated for each zone and listed in Table 3.3. [12] reported the highest 'H' value for the Indo-Burma subduction zone, which our study also observed for the Indo-Burma seismic thrust zone (IBSTZ). Differences in 'H' values between [12] and the present chapter are likely due to variations in methods and earthquake catalog durations.

Table 3.3. The most probable largest annual magnitude (H) for four distinct seismic zones.

S. No	Seismic Zone	α	β	Most probable maximum annual magnitude (H)
1	NEHSZ	26915.3	1.91	5.3
2	SZSZ	97723.7	2.09	5.4
3	BSSZ	6760.8	1.86	4.7
4	IBSTZ	169824.3	2.17	5.5

Likewise, Table 3.4 presents the estimated most probable maximum magnitudes (H(t)) for various time periods in the four seismic zones, calculated using equation 13 (as mentioned in chapter 2). [31] reported an H(t) of approximately 8.5 over fifty years for northeast India, while [32] estimated it at 8.6. [12] reported 7.3, and [12] found a more than 50% probability for an earthquake magnitude of 7 or greater over fifty years. Our study found an H(t) of 7.39 for fifty years, consistent with [12]. Northeast India hasn't experienced an earthquake over M_W 8.5 since the 1950 Assam earthquake (M_W 8.6), indicating the elapsed T(m) estimated by earlier studies. However, a M_W 6.9 earthquake on September 18, 2011, provides recent insights into regional seismic activity [33].

Table 3.4. The most probable largest magnitude (H(t)) for four distinct seismic zones over different period.

		NEHSZ	SASZ	BSSZ	IBSTZ
S. No	**Time (year)**	**H(t)**	**H(t)**	**H(t)**	**H(t)**
1	1	5.35	5.5	4.75	5.55
2	10	6.55	6.6	5.98	6.62
3	20	6.91	6.94	6.36	6.94
4	30	7.13	7.13	6.57	7.12
5	40	7.28	7.27	6.73	7.25
6	50	7.39	7.37	6.85	7.36
7	60	7.49	7.46	6.95	7.44
8	70	7.57	7.54	7.03	7.51
9	80	7.64	7.6	7.1	7.57
10	90	7.7	7.66	7.17	7.63
11	100	7.76	7.71	7.22	7.68

The H(t) over different period for four distinct seismic zones are illustrated in Figure 3.7.

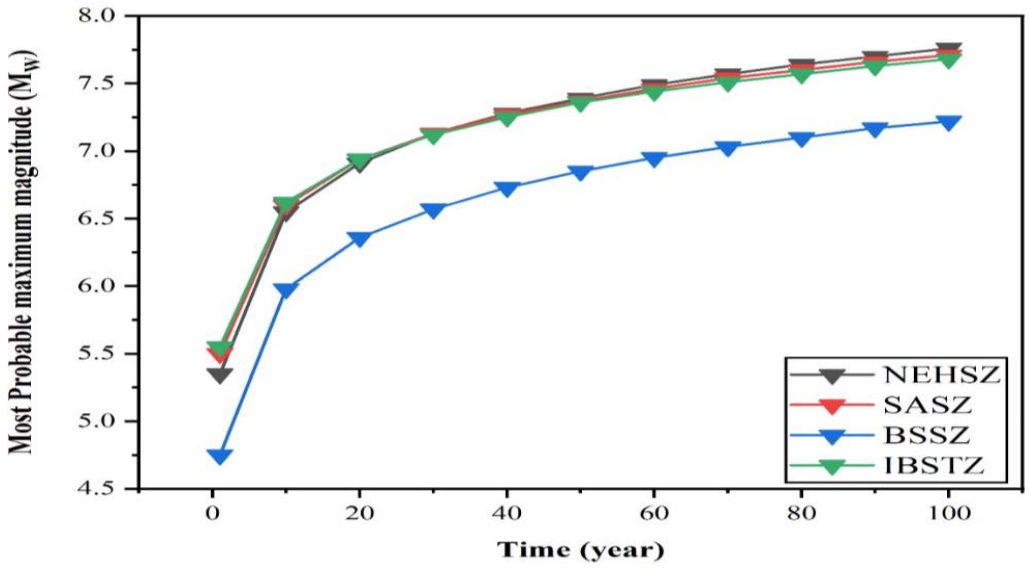

Figure 3.7. The most probable maximum magnitude versus Time for four distinct seismic zones.

3.6.3. Return period (T(m))

Gumbel EVT can estimate the T(m) of extreme events using equation 14 (as mentioned in chapter 2). Table 3.5 lists T(m) for magnitudes 4 to 8.5 across four seismic zones. It shows that T(m) is shorter for the Indo-Burma seismic thrust zone (IBSTZ) compared to NEHSZ, BSSZ, and SASZ. The T(m) order for magnitudes 4.0 to 6.5 is IBSTZ < SASZ < NEHSZ < BSSZ, and for 7.0 to 8.5, it's SASZ < IBSTZ < NEHSZ < BSSZ. [34] reported a T(m) of 5 to 7 years for a magnitude 6 earthquake in the Arakan-Yoma subduction zone. Thingbaijam and Nath (2008) found the T(m) for MW ≥ 8.0 follows SHZ < EHZ < MBZ < EBZ. [12] and [2] also reported shorter T(m) for the Arakan-Yoma subduction zone compared to other zones.

Table 3.5. The T(m) of different magnitudes for four seismic zones.

	NEHSZ	**SASZ**	**BSSZ**	**IBSTZ**
Magnitude	RT (year)	RT (year)	RT (year)	RT (year)
4	0.078	0.044	0.252	0.035
4.5	0.201	0.125	0.639	0.103
5	0.522	0.354	1.618	0.304
5.5	1.357	1.006	4.101	0.899
6	3.524	2.858	10.393	2.658
6.5	9.158	8.127	26.341	7.866
7	23.797	23.107	66.76	23.278
7.5	61.84	65.701	169.203	68.888
8	160.702	186.812	428.847	203.87
8.5	417.61	531.18	1086.916	603.34

The T(m) versus magnitude plot is shown in Figure 3.8. From Figure 3.8 it can be inferred that the T(m) for magnitude $M_W = 6.0$ is small for IBSTZ but for $M_W > 6.5$, SASZ has the smallest T(m). Thus, it can be inferred that SASZ is more prone to seismic hazard due to small T(m) for large magnitude earthquakes.

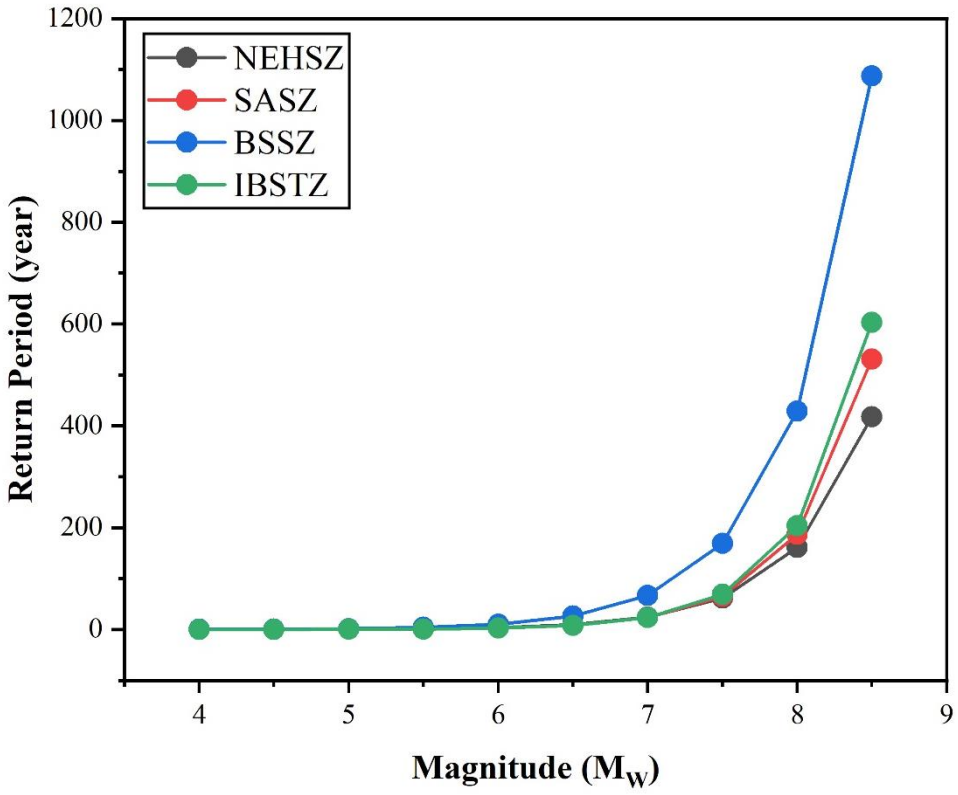

Figure 3.8. The T(m) versus magnitude plot for four distinct seismic zones.

3.6.4. Estimation of probability of occurrence of different magnitude (P(t))

To evaluate the likelihood of earthquakes of different magnitudes over specific time periods in the four seismic zones, we used equation 15 (as mentioned in chapter 2). This method provides insights into the probability distribution of earthquake magnitudes over various time frames. Table 3.6 shows the probabilities of earthquakes ranging from magnitude 4.0 to 8.5 occurring over 1 to 100 years in the North-Eastern Himalayan Seismic Zone (NEHSZ). Analysis of Figure 3.9 and Table 3.6 indicates a 100% likelihood of an earthquake with $M_W \leq 6$ occurring in the NEHSZ within the next fifty years, consistent with [2]. However, the probability for higher magnitudes, such as M_W 8.0 and 8.5, is lower. [12] also noted a decreasing probability for earthquakes with $M_W \geq 6.5$ over the next fifty years. Extending the time frame to a hundred years increases the probability for earthquakes with magnitudes M_W 7.0 to 8.0, due to multiple such events in the past century. However, the likelihood of an M_W 8.5 earthquake within the next hundred years remains below fifty percent, with T(m) analysis suggesting it may occur after over four hundred years. These findings align with existing studies on the NEHSZ.

Table 3.6. The probability of occurrences for different magnitude over different period for NEHSZ.

M_W	P_1	P_{10}	P_{20}	P_{30}	P_{40}	P_{50}	P_{60}	P_{70}	P_{80}	P_{90}	P_{100}
4	1	1	1	1	1	1	1	1	1	1	1
4.5	0.993	1	1	1	1	1	1	1	1	1	1
5	0.853	1	1	1	1	1	1	1	1	1	1
5.5	0.522	0.999	1	1	1	1	1	1	1	1	1
6	0.247	0.941	0.997	1	1	1	1	1	1	1	1
6.5	0.103	0.664	0.887	0.962	0.987	0.996	0.999	1	1	1	1
7	0.041	0.343	0.568	0.717	0.814	0.878	0.92	0.947	0.965	0.977	0.985
7.5	0.016	0.149	0.276	0.384	0.476	0.554	0.621	0.678	0.726	0.767	0.802
8	0.006	0.06	0.117	0.17	0.22	0.267	0.312	0.353	0.392	0.429	0.463
8.5	0.002	0.024	0.047	0.069	0.091	0.113	0.134	0.154	0.174	0.194	0.213

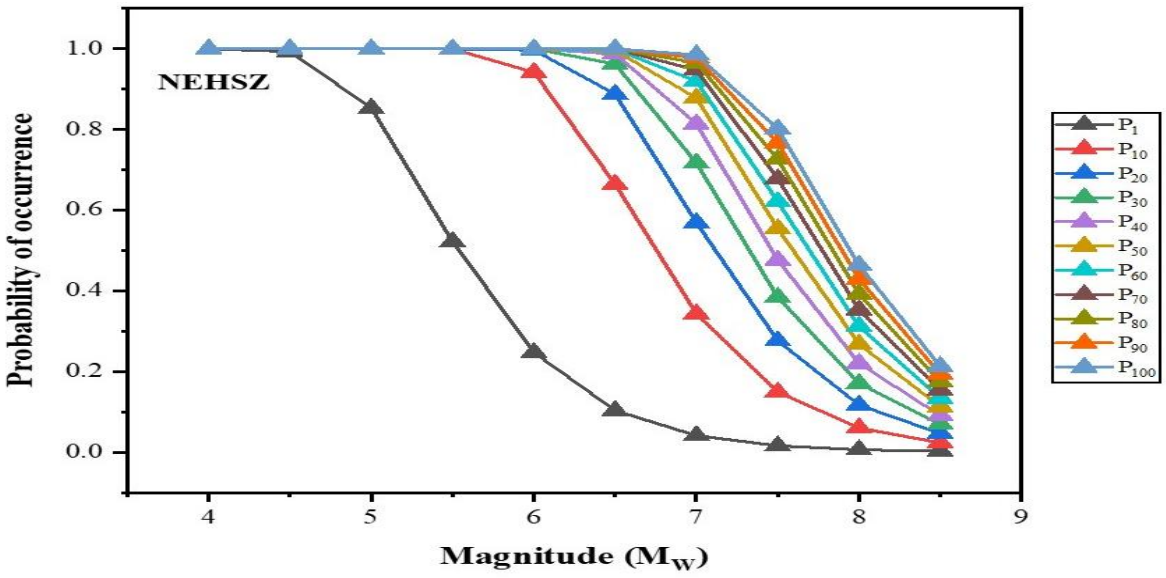

Figure 3.9. The probability of occurrence versus magnitude plot for NEHSZ.

Likewise, Table 3.7 presents the likelihood of occurrence of earthquakes with magnitudes varying from M_W 4.0 to 8.5 occurring over the next 1 to 100 years for SASZ, while Figure 3.10 visualizes these probabilities. The probability analysis for SASZ indicates a 100 percent probability of earthquakes with magnitudes $M_W \leq 6.0$ occurring over the next fifty

years. Conversely, the probability of larger magnitude earthquakes (M_W 8.0 to 9.0) decreases exponentially.

Table 3.7. The probability of occurrences for different magnitude over different period for SASZ.

M_W	P_1	P_{10}	P_{20}	P_{30}	P_{40}	P_{50}	P_{60}	P_{70}	P_{80}	P_{90}	P_{100}
4	1	1	1	1	1	1	1	1	1	1	1
4.5	1	1	1	1	1	1	1	1	1	1	1
5	0.941	1	1	1	1	1	1	1	1	1	1
5.5	0.63	1	1	1	1	1	1	1	1	1	1
6	0.295	0.97	0.999	1	1	1	1	1	1	1	1
6.5	0.116	0.708	0.915	0.975	0.993	0.998	0.999	1	1	1	1
7	0.042	0.351	0.579	0.727	0.823	0.885	0.925	0.952	0.969	0.98	0.987
7.5	0.015	0.141	0.262	0.367	0.456	0.533	0.599	0.655	0.704	0.746	0.782
8	0.005	0.052	0.102	0.148	0.193	0.235	0.275	0.313	0.348	0.382	0.415
8.5	0.002	0.019	0.037	0.055	0.073	0.09	0.107	0.123	0.14	0.156	0.172
9	0.001	0.007	0.013	0.02	0.026	0.033	0.039	0.045	0.052	0.058	0.064

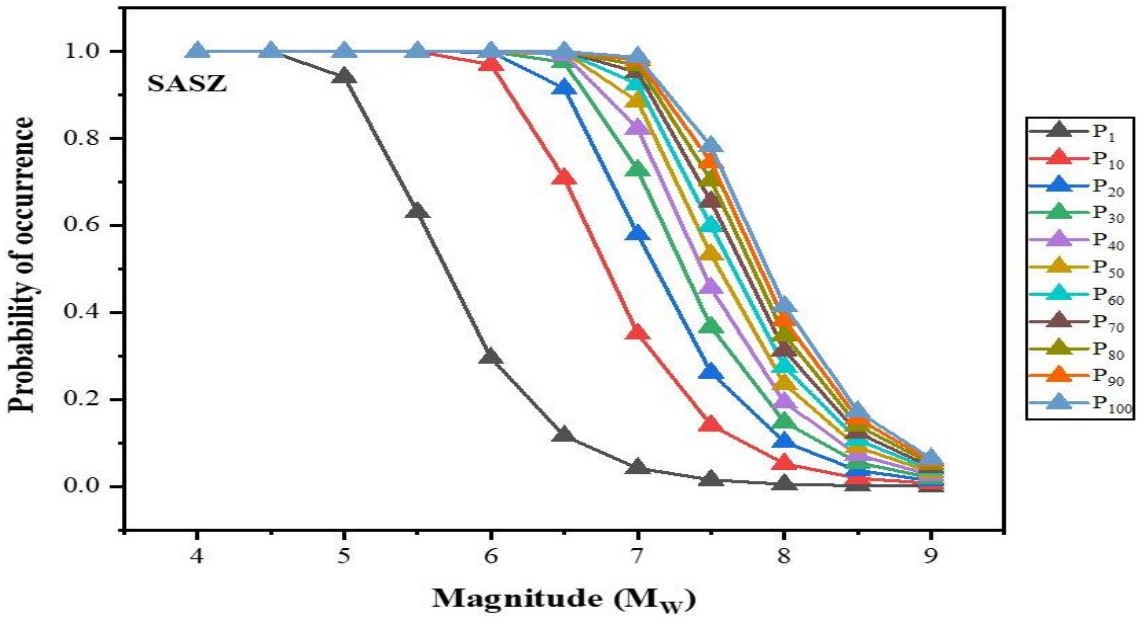

Figure 3.10. The probability of occurrence versus magnitude plot for SASZ.

Furthermore, Table 3.8 provides the probabilities of earthquakes occurring over different time periods in the BSSZ, while Figure 3.11 visualizes these probabilities. Based on the probability analysis, it is predicted that within the next fifty years, there is a 100 percent chance of earthquakes occurring within the magnitude range of M_W 4.0 to 5.5 in the studied region (BSSZ). This indicates a high likelihood of seismic activity in that specific magnitude range over the given time frame. However, the likelihood of larger magnitude earthquakes decreases exponentially. Furthermore, over the next 100 years, there is a probability of more than fifty percent for earthquakes with magnitudes varying from M_W 4.0 to 7.0, while the probability of earthquakes with magnitudes from M_W 7.5 to 8.5 is less than fifty percent. Consequently, we can expect a higher occurrence of small and intermediate earthquakes, ranging from M_W 4.0 to 6.5, compared to larger magnitude earthquakes in the next hundred years.

Table 3.8. The probability of occurrences for different magnitude over different period for BSSZ.

M_W	P_1	P_{10}	P_{20}	P_{30}	P_{40}	P_{50}	P_{60}	P_{70}	P_{80}	P_{90}	P_{100}
4	0.981	1	1	1	1	1	1	1	1	1	1
4.5	0.791	1	1	1	1	1	1	1	1	1	1
5	0.461	0.998	1	1	1	1	1	1	1	1	1
5.5	0.216	0.913	0.992	0.999	1	1	1	1	1	1	1
6	0.092	0.618	0.854	0.944	0.979	0.992	0.997	0.999	1	1	1
6.5	0.037	0.316	0.532	0.68	0.781	0.85	0.897	0.93	0.952	0.967	0.978
7	0.015	0.139	0.259	0.362	0.451	0.527	0.593	0.65	0.698	0.74	0.776
7.5	0.006	0.057	0.111	0.162	0.211	0.256	0.299	0.339	0.377	0.413	0.446
8	0.002	0.023	0.046	0.068	0.089	0.11	0.131	0.151	0.17	0.189	0.208
8.5	0.001	0.009	0.018	0.027	0.036	0.045	0.054	0.062	0.071	0.079	0.088

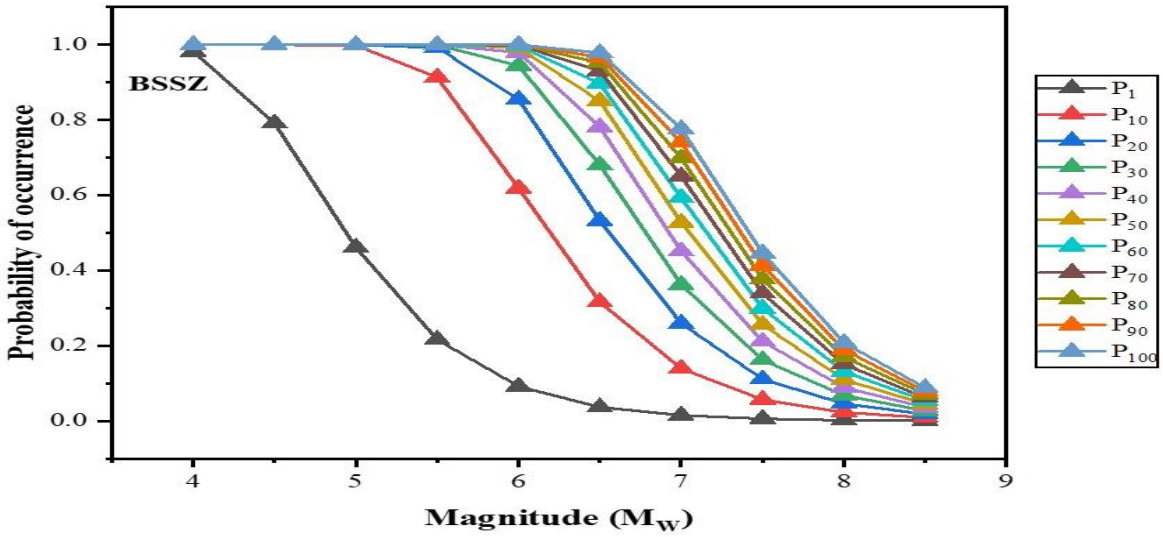

Figure 3.11. The probability of occurrence versus magnitude plot for BSSZ.

Table 3.9 presents the probabilities of different magnitudes occurring in the Indo-Burma seismic thrust zone (IBSTZ) over the next hundred years, while Figure 3.12 graphically represents these probabilities. The probability of an earthquake with $M_W \leq 6.0$ occurring in the next fifty years is 100 percent. Furthermore, there is a probability of more than fifty percent for earthquakes with magnitudes varying from M_W 4.0 to 7.5 in the next hundred years. However, the probability of larger magnitude earthquakes in the range of M_W 8.0 to 8.5 remains below fifty percent over the next hundred years.

Table 3.9. The probability of occurrences for different magnitude over different period for IBSTZ.

M_W	P_1	P_{10}	P_{20}	P_{30}	P_{40}	P_{50}	P_{60}	P_{70}	P_{80}	P_{90}	P_{100}
4	1	1	1	1	1	1	1	1	1	1	1
4.5	1	1	1	1	1	1	1	1	1	1	1
5	0.963	1	1	1	1	1	1	1	1	1	1
5.5	0.672	1	1	1	1	1	1	1	1	1	1
6	0.314	0.977	0.999	1	1	1	1	1	1	1	1
6.5	0.119	0.72	0.921	0.978	0.994	0.998	1	1	1	1	1
7	0.042	0.349	0.577	0.724	0.821	0.883	0.924	0.951	0.968	0.979	0.986
7.5	0.014	0.135	0.252	0.353	0.44	0.516	0.581	0.638	0.687	0.729	0.766
8	0.005	0.048	0.093	0.137	0.178	0.217	0.255	0.291	0.325	0.357	0.388
8.5	0.002	0.016	0.033	0.049	0.064	0.08	0.095	0.11	0.124	0.139	0.153

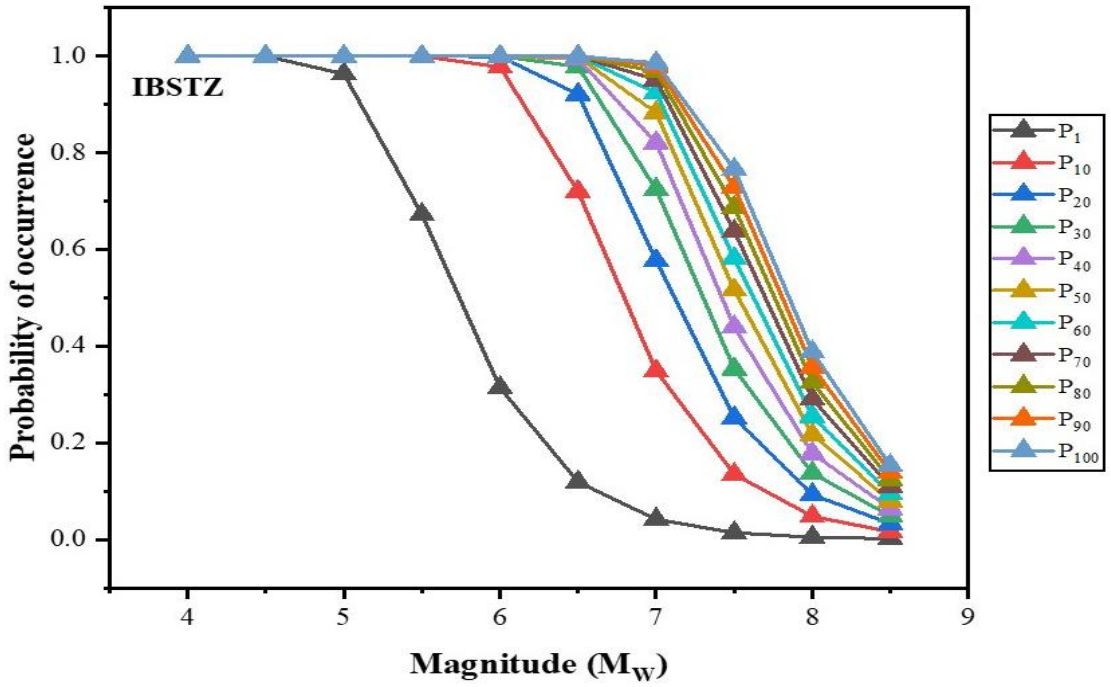

Figure 3.12. The probability of occurrence versus magnitude plot for IBSTZ.

The comparative analysis of the probabilities of different magnitude earthquakes in the Four Tectonic Segments reveals some interesting findings. The possibility of earthquakes with $M_W \leq 6.0$ occurring in the next fifty years is a hundred percent for NEHSZ, SASZ, and IBSTZ. However, the probability of higher magnitude earthquakes decreases exponentially for all the zones. Additionally, the probability of earthquakes with $M_W \geq 7.0$ in the next fifty years follows the order SASZ > IBSTZ > NEHSZ > BSSZ. Furthermore, in the next hundred years, the order of probability for an $M_W = 8.5$ earthquake is NEHSZ > SASZ > IBSTZ > BSSZ. Based on these results, it can be inferred that NEHSZ and SASZ are the most favourable seismic zones for the occurrence of an $M_W = 8.5$ earthquake in the next hundred years. Moreover, the maximum magnitude values (Mmax) obtained using different methodologies are 8.6 for SASZ and 8.5 for NEHSZ. Given that the Mmax value for SASZ is higher than that of NEHSZ, we can conclude that among the four seismic zones, SASZ poses a greater seismic hazard.

3.7. References

[1] Bureau of Indian Standard. Indian standard, criteria for earthquake resistance design of structures. 5th revision, I. New Delhi, India: Author; 2002.

[2] Baro, O. and Kumar, A. Seismic source characterization for the Shillong Plateau in Northeast India. *Journal of Seismology,* 21(5):1229-49, 2017.

[3] Bilham, R. Earthquakes in India and the Himalaya: tectonics, geodesy and history. *Annals of Geophysics,* 47(2-3):839-58, 2004.

[4] Kayal, J. R. Himalayan tectonic model and the great earthquakes: an appraisal. *Geomatics, Natural Hazards and Risk,*1(1):51-67, 2010.

[5] Borah, N., Kumar, A. and Dhanotiya, R. Seismic source zonation for NE India on the basis of past EQs and spatial distribution of seismicity parameters. *Journal of Seismology, 2*5(6):1483-506, 2021.

[6] Ni, J. and Barazangi, M. Seismotectonics of the Himalayan collision zone: geometry of the under thrusting Indian plate beneath the Himalaya. *Journal of Geophysical Research,* 89(B2):1147-63, 1984.

[7] Mullick, M. and Mukhopadhyay, D. Kinematics of faults in Bengal Basin: constraints from GPS measurements. *Geodesy and Geodynamics,*11(4):242-51, 2020.

[8] Sitharam, T. G. and Sil, A. Comprehensive seismic hazard assessment of Tripura and Mizoram states. *Journal of Earth System Science,* 123(4):837-57, 2014.

[9] Reasenberg, P. A. Second order moment of central California seismicity, 1969-1982. *Journal of Geophysical Research,* 90(B7):5479-95, 1985.

[10] Gupta, I. D. Delineation of probable seismic sources in India and neighbourhood by a comprehensive analysis of seismotectonic characteristics of the region. *Soil Dynamics and Earthquake Engineering,* 26(8):766-90, 2006.

[11] Sharma, M. and Malik, S. Probabilistic seismic hazard analysis and estimation of spectral strong ground motion on bed rock in north East India. *International conference on earthquake engineering*, Taipei, Taiwan (2006).

[12] Yadav, R. B. S., Tripathi, J. N., Shanker, D., Rastogi, B. K., Das, M. C. and Kumar, V. Probabilities for the occurrences of medium to large earthquakes in Northeast India and adjoining region. *Natural Hazards,* 56(1):145-67, 2011.

[13] Kolathayar, S. and Sitharam, T. G. Characterization of regional seismic source zones in and around India. *Seismological Research Letters,* 83(1):77-85, 2012.

[14] Pallav, K., Raghukanth, S. T. G. and Singh, K. D. Probabilistic seismic hazard estimation of Manipur, India. *Journal of Geophysics and Engineering,* 9(5):516-33, 2012.
[15] Das, R., Sharma, M. L. and Wason, H. R. Probabilistic seismic hazard assessment for northeast India region. *Pure and Applied Geophysics,* 173(8):2653-70, 2016.
[16] Bahuguna, A., and Sil, A. Comprehensive Seismicity, Seismic Sources and Seismic Hazard Assessment of Assam, North East India. *Journal of Earthquake Engineering*, *24*(2): 254–297, 2018.
[17] Lallawmawma, C., Sharma, M. L. and Das, J. D. Probabilistic seismic hazard and risk assessment of Mizoram, North East India. *Natural Hazards Research,* 3(3): 447-463, 2023.
[18] Banerjee, P., Bürgmann, R., Nagarajan, B. and Apel, E. Intraplate deformation of the Indian subcontinent. *Geophysical Research Letters,* 35(18):1-5, 2008.
[19] Vernant, P., Bilham, R., Szeliga, W., Drupka, D., Kalita, S. and Bhattacharyya, A. K. et al. Clockwise rotation of the Brahmaputra valley relative to India: tectonic convergence in the Eastern Himalaya, Naga Hills, and Shillong Plateau. *Journal of Geophysical Research: Solid Earth,* 119(8):6558-71, 2014.
[20] Barman, P., Jade, S., Shrungeshwara, T. S., Kumar, A., Bhattacharyya, S. and Ray, J. D. et al. Crustal deformation rates in Assam Valley, Shillong Plateau, Eastern Himalaya, and Indo-Burmese region from 11 years (2002-2013) of GPS measurements. *International Journal of Earth Sciences,* 106(6):2025-38, 2017.
[21] Kayal, J. R. Microearthquake seismology and Seismotectonics of South Asia. New York, India: McGraw-Hill, 2008.

[22] Kundu, B. and Gahalaut, V. K. Tectonic geodesy revealing geodynamic complexity of the Indo-Burmese arc region. *North-East India: Current Science,* 104: 920–933, 2013.
[23] Oryan, B., Betka, P. M., Steckler, M. S., Nooner, S. L., Lindsey, E. O. and Mondal, D. et al. New GNSS and geological data from the Indo-Burman subduction zone indicate active convergence on both a locked megathrust and the Kabaw Fault. *Journal of Geophysical Research: Solid Earth,* 128(4): 2023.
[24] Wiemer, S. and Wyss, M. Minimum magnitude of completeness in earthquake catalogs: examples from Alaska, the Western United States, and Japan. *Bulletin of the Seismological Society of America,* 90(4):859-69, 2000.
[25] Woessner, J. and Wiemer, S. Assessing the quality of earthquake catalogues: estimating the magnitude of completeness and its uncertainty. *Bulletin of the Seismological Society of America,* 95(2):684-98, 2005.

[26] Stepp, J. C. Analysis of completeness of the earthquake sample in the Puget Sound area and its effect on statistical estimates of earthquake hazard. *Proceeding of the International conference on microzonation*, Seattle, USA 2:897-910, 1972.
[27] Gutenberg, B. and Richter, C. F. Frequency of Earthquakes in California. *Bulletin of the Seismological Society of America,* 34(4): 185-188, 1944.
[28] Kijko, A., Smit, A. and Sellevoll, M. A. Estimation of earthquake hazard parameters from incomplete data files. Part III. Incorporation of uncertainty of earthquake-occurrence model. *Bulletin of the Seismological Society of America,* 106(3): 1210-22, 2016.
[29] National Disaster Management Authority (NDMA). Development of probabilistic seismic hazard map of India. *Technical report by national disaster management authority.* Government of India, 2010.
[30] Thingbaijam, K. K. S. and Nath, S. K. Estimation of maximum earthquakes in Northeast India. *Pure and Applied Geophysics,* 165(5):889-901, 2008.
[31] Rao, P. S. and Rao, B. R. Estimated earthquake probabilities in the Northeast India and Andaman-Nicobar Island. *Mausam,* 550(341): 267–273, 1979.
[32] Goswami, H. C. and Sarmah, S. K. A comparison of the estimated earthquake probabilities in the northeast Indian region. *Tectonophysics,* 95(1-2): 91-9, 1983.

[33] Baruah, S., Saikia, S., Baruah, S., Bora, P. K., Tatevossian, R. and Kayal, J. R. The September 2011 Sikkim Himalaya earthquake Mw 6.9: is it a plane of detachment earthquake? *Geomatics, Natural Hazards and Risk,* 7(1): 248–263, 2016.
[34] Shanker, D. and Sharma, M. L. Estimation of seismic hazard parameters for the Himalayas and its vicinity from complete data files. *Pure and Applied Geophysics,* 152(2): 267–279, 1998.